ORIGINAL ARTICLE

Design, Synthesis, Characterization and Evaluation of Anticancer Activity of Substituted-4-(Substitutedphenylhydrazono)-3,4-Dihydroquinolin-2-(1H)-One

Swezel Negredo[1], Bheemanagouda Biradar[2], SoniyaNaik Phadte[1], Sunil Shingade[3], Manjunath Katagi[4], Shivalingrao Mamle Desai[4], Prashant Yuvaraj Mali[5]

[1]Department of Pharmaceutical Chemistry, P.E.S's Rajaram and Tarabai Bandekar College of Pharmacy, Ponda, Goa, India, [2]Department of Pharmacology, P.E.S's Rajaram and Tarabai Bandekar College of Pharmacy, Ponda, Goa, India, [3]Department of Pharmaceutical Chemistry, V. P. College of Pharmacy, Sindhudurg, Maharashtra, India, [4]Department of Pharmaceutical Chemistry, Bapuji College of Pharmacy, Davangere, Karnataka, India, [5]Department of Pharmacology and Pharmacy Practice, Yashwantrao Bhonsale College of Pharmacy, Sindhudurg, Maharashtra, India

Abstract

Background: Hepatocellular carcinoma (HCC) remains a therapeutically challenging malignancy due to limited treatment options and toxicity associated with current chemotherapeutic and targeted agents. The current investigation deals with the design, synthesis, characterization, *in silico* studies of a series of 4- (2-substitutedphenylhydrazono)-6-substituted-3,4-dihydroquinolin-2(1*H*)-one derivatives and screening for their *in vitro* anticancer activity against HCC by sulforhodamine B assay. **Materials and Methods:** All the synthesised compounds were characterised by ultraviolet-visible, Fourier transform infrared, nuclear magnetic resonance (^{1}H and ^{13}C) and mass spectroscopy. **Results and Discussion:** Docking studies of all the synthesized compounds revealed favorable docking score utilising the epidermal growth factor receptor (EGFR)-tyrosine kinase binding site (Protein Data Bank: 1m17), with compound 4-(2-(2,4-dinitrophenyl)hydrazono)-6-fluoro-3,4-dihydroquinolin-2(1*H*)-one (IIIc_4) showing the highest molecular docking (MolDock) score of −104.42, which is comparable to reference drug Imatinib with a MolDock score of −109.39 and found to be more effective than standard drug Adriamycin which showed MolDock score of −76.67. Among the screened derivatives, three of the derivatives, that is, compound 4-(2-(2,4-dinitrophenyl)hydrazono)-3,4-dihydroquinolin-2(1*H*)- one (IIIa_4); 6-chloro-4- (2-(2,4-dinitrophenyl) hydrazono)-3,4-dihydroquinolin-2 (1*H*)-one (IIIb_4) and 4-(2-(2,4- dinitrophenyl)hydrazono)-6-fluoro-3,4-dihydroquinolin-2(1*H*)-one (IIIc_4), had an inhibitory effect on cell growth with GI50 <10 µg/mL when compared to positive control Adriamycin. **Conclusion:** The combined computational and biological data suggest that these hydrazinoquinoline derivatives, especially those with electron-withdrawing substituents, hold promise as lead structures for further development in liver cancer therapy targeting EGFR. Future studies would focus on their detailed mechanism, selectivity, and *in vivo* efficacy to validate their therapeutic utility.

Key words: Anticancer, hepatocellular carcinoma G2 cell line, human hepatocellular carcinoma, quinolin-2-one, sulforhodamine B

INTRODUCTION

Hepatocellular carcinoma (HCC) remains a therapeutically challenging malignancy due to limited treatment options and the toxicity associated with current chemotherapeutic and targeted agents.[1] Among the molecular targets implicated in HCC progression, epidermal growth factor receptor tyrosine kinase (EGFR-TK) plays a critical

Address for correspondence:
Bheemanagouda Biradar, Department of Pharmacology, P.E.S's Rajaram and Tarabai Bandekar College of Pharmacy, Ponda, Goa, India. Mobile: +91-8554812734.
E-mail: rajubiradar3107@gmail.com

Received: 17-05-2026
Revised: 21-06-2026
Accepted: 27-06-2026

role in regulating aberrant cell proliferation and survival pathways. Although several EGFR inhibitors have been clinically developed, their utility in liver cancer is restricted by adverse hepatic effects and the emergence of resistance, underscoring the need for structurally novel EGFR-targeted chemotypes with improved efficacy and safety.[2,3] Quinolin-2-one derivatives represent a privileged heterocyclic framework in medicinal chemistry and have been extensively explored for kinase inhibition and anticancer activity. Both naturally occurring and synthetic quinolinone analogs exhibit favorable pharmacological profiles, attributable to their structural flexibility and ability to participate in key hydrogen-bonding and π-π stacking interactions within enzyme active sites.[4,5] In parallel, hydrazone moieties are well recognised for their role in enhancing biological activity through increased conformational adaptability and strong donor-acceptor interactions, making them valuable structural motifs in anticancer drug design.[6,7]

In the present study, a rational design strategy was employed to integrate the quinolin-2-one core with substituted phenylhydrazone functionalities to generate a new class of EGFR-targeting molecules. The innovation of this work lies in the systematic modification of the quinolinone scaffold at the 4- and 6-position to fine-tune electronic properties and binding interactions. Introduction of a hydrazone linkage at the 4-position was designed to enhance ligand–receptor hydrogen bonding within the EGFR kinase domain, while halogen substitution (Cl/F) at the 6-position was intended to modulate lipophilicity and electronic distribution. In addition, incorporation of electron-withdrawing groups, particularly ortho and para-dinitro substituents on the phenylhydrazone ring, was hypothesised to strengthen binding affinity and improve antiproliferative activity. This chemical innovation is supported by an integrated workflow combining synthesis, spectroscopic characterization, molecular docking (MolDock), absorption, distribution, metabolism, and excretion (ADME) prediction, and *in vitro* anticancer evaluation. MolDock against the EGFR-TK domain (Protein Data Bank [PDB] ID: 1M17) was employed to establish structure–binding relationships and to guide biological interpretation. The designed hydrazono-quinolinone derivatives represent a structurally distinct chemotype compared to conventional EGFR inhibitors, offering new insights into scaffold modification for kinase-targeted anticancer agents. Accordingly, this study reports the design, synthesis, and evaluation of a series of 4-(substitutedphenylhydrazono)-6-substituted-3,4-dihydroquinolin-2(1*H*)-one derivatives as potential EGFR-directed anticancer agents against HCC.

MATERIALS AND METHODS

Chemicals

The chemicals were procured from reputable suppliers, including Sigma-Aldrich, NICE Chemicals, S. D. Fine-Chem Ltd., Mumbai and Spectrochem Pvt. Ltd., Mumbai.

Instruments and equipment's

Melting points of synthesised compounds were determined by Thiele's melting point apparatus and are uncorrected. λ max of every step compound was determined by a ultraviolet-visible spectrophotometer 1800 model, and IR absorbance bands were determined by a SHIMADZU FT-IR AFFINITY-1 spectrophotometer by using KBr pellets. The proton nuclear magnetic resonance (^{1}H NMR) and carbon-13 nuclear magnetic resonance (^{13}C NMR) spectral data of the synthesised compounds were recorded on a Bruker advance II 400 NMR spectrophotometer using $CDCl_3$/dimethyl sulfoxide-d6 (DMSO-*d6*) solvent and TMS as internal standard, chemical shifts are expressed as delta (δ) values (ppm). The mass spectra were recorded on waters, quadrupole time-of-flight micromass liquid chromatography-mass spectrometry and expressed as mass to charge ratio (m/z).

Synthesis of 6-substituted quinolin-2,4(1*H*,3*H*)-dione [IIa/IIb/IIc]

Solution of 4-hydroxyquinolin-(1*H*)-one (Ia/b/c) was prepared in acetic acid by cooling at 5°C. The solution of chromium trioxide (0.42 mol;42 g) was also prepared by mixing in 70 mL of water and 30 mL of acetic acid; the obtained solution was mixed with (Ia/b/c) by maintaining the solution below 100°C temperature. Stirred for 2 h, and the precipitate obtained was filtered, washed repeatedly with cold water. The completion of the reaction was confirmed by thin-layer chromatography (TLC) using *n*-Hexane: Ethylacetate as mobile phase in the ratio of 6:4.

Quinolin-2,4(1H,3H)-dione (IIa)

UV-Visible data (λmax, nm): 256.60; infrared (IR) data (KBr, cm^{-1}): 3273.20 (-NH stretch); 3093.82 (-Aromatic -CH stretch); 1701.22 (-C=O stretch of ketone) 1658.78 (-C=O stretch of amide); ^{1}H NMR data (δ ppm, DMSO-d_6): 7.78–7.11 (m, 4H, Ar-H); 5.74 (s, 1H, NH); 5.38 (s, 2H, -CH_2 quinolone).

6-chloroquinolin-2,4(1H,3H)-dione (IIb)

UV-Visible data (λmax, nm): 254.30**;**IR data (KBr, cm^{-1}): 3120.82 (-NH stretch); 3084.18 (-Aromatic -CH stretch); 1660.71 (-C=O stretch of amide) 675.09 (-C-Cl stretch); ^{1}H NMR data (δ ppm, DMSO-d_6): 8.33–7.64 (m, 3H, Ar-H); 4.67 (s, 1H, NH); 3.47 (s, 2H, -CH2 quinolone).

6-Flouroquinolin-2,4(1H,3H)-dione (IIc)

UV-Visible data (λmax, nm): 213.58; IR data (KBr, cm^{-1}): 3340.56 (-NH stretch); 3047.56 (-Aromatic -CH stretch); 1657.56 (-C=O stretch of amide); 1127.65 (-C-F stretch); ^{1}H NMR data (δ ppm, DMSO-d_6): 7.90-6.57 (m, 3H, Ar-H); 4.02 (s, 1H, NH); 3.52 (s, 2H, -CH2 quinolone).

Synthesis of 4-[(substitutedphenyl)hydrazono]-6-substituted-3,4-dihydroquinolin2-(1*H*)-one [IIIa-(1-4)/IIIb-(1-4)/IIIc-(1-4)]

To substitute phenylhydrazine (2.52 mmol), 1 mL of concentrated hydrochloric acid, 6- substituted/unsubstituted-3,4-dihydroquinolin-2-(1*H*)-one (1.15 mmol), ethanol was added and refluxed for 5 min, cooled, the obtained solid was filtered and recrystallized. The reaction was monitored by TLC using *n*-Hexane: Ethylacetate in the ratio of 6:4. The compounds synthesised in this manner are shown in [Table 1] along with their physical data.

4-(2-Phenylhydrazono)-3,4-dihydroquinolin-2(1H)-one (IIIa_1)

UV-Visible data (λmax, nm): 258.30; IR data (KBr, cm^{-1}): 3278.99 (-NH stretch); 3207.62 (-NH stretch of phenylhydrazone); 2949.16 (Aromatic -CH stretch); 1668.43 (-C=O stretch of amide); ^{1}H NMR data (δ ppm, DMSO-d_6): 10.26 (s, 1H, phenylhydrazone -NH); 8.26–7.00 (m, 4H, Ar-H); 5.89 (s, 1H, NH); 5.32 (s, 2H, -CH2 quinolone).

Elemental analysis: $C_{15}H_{13}N_3O$: Calculated: C, 71.70; H, 5.21; N, 16.72; O, 6.37; Found: C, 71.34; H, 5.19; N, 16.45; O, 6.34.

4-(2-(3-Fluorophenyl)hydrazono)-3,4-dihydroquinolin- 2(1H)-one (IIIc_1)

UV-Visible data (λmax, nm): 258.80; IR data (KBr, cm^{-1}): 3277.06 (-NH stretch); 3215.34 (-NH stretch of phenylhydrazone); 2949.16, 2906.73, 2862.36, 2821.86, 2758.21, 2702.27 (-Aromatic -CH stretch); 1662.64 (-C=O stretch of amide); 1631.78 (-C=N stretch); ^{1}H NMR data (δ ppm, DMSO-d_6): 10.26 (s, 1H, phenylhydrazone -NH); 7.78–7.11 (m, 8H, Ar-H); 5.74 (s, 1H, NH); 5.34 (s, 2H, -CH2).

Elemental analysis: $C_{15}H_{12}FN_3O$: Calculated: C, 66.91; H, 4.49; F, 7.06; N, 15.60; O, 5.94; Found: C, 66.23; H, 4.27; F, 7.23; N, 15.23; O, 5.02.

4-(2-(3-Nitrophenyl)hydrazono)-3,4-dihydroquinolin- 2(1H)-one (IIIa_3)

UV-Visible data (λmax, nm): 258.60; IR data (KBr, cm^{-1}): 3344.57 (-NH stretch); 3288.63 (-NH stretch of phenylhydrazone); 2949.16, 2902.87, 2860.43, 2823.79, 2754.35, 2715.77 (-Aromatic -CH stretch); 1668.43 (-C=O stretch of amide); 1633.71 (-C=N stretch); ^{1}H NMR data (δ ppm, DMSO-d_6): 8.92 (s, 1H, phenylhydrazone -NH); 7.84–7.13 (m, 8H, Ar-H); 5.81 (s, 1H, NH); 5.38 (s, 2H, -CH2). ^{13}C NMR data (δ ppm, DMSO-d_6): 163.48 (1C, C=O); 162.36 (1C, C=N); 148.20 (1C, C-NO_2); 146.99 (1C, Ar-C-NH); 139.05-107.85 (10C, Ar-C); 98.12 (1C, -CH_2).

Elemental analysis: $C_{15}H_{12}N_4O_3$: Calculated: C, 60.81; H, 4.08; N, 18.91; O, 16.20; Found: C, 60.56; H, 4.00; N, 18.78; O, 16.05.

4-(2-(2,4-Dinitrophenyl) hydrazono)-3,4- dihydroquinolin-2(1H)-one (IIIa_4)

UV-Visible data (λmax, nm): 258.90; IR data (KBr, cm^{-1}): 3325.28 (-NH stretch of phenylhydrazone); 3128.54 (-NH stretch);3088.03, 2949.16, 2904.80, 2856.58 (Aromatic -CH stretch); 1668.43 (-C=O stretch of amide); 1631.78 (-C=N stretch); ^{1}H NMR data (δ ppm, DMSO-d_6): 9.99 (s, 1H, phenylhydrazone -NH); 8.82–7.13 (m, 7H, Ar H); 5.74 (s, 1H, NH); 5.32 (s, 2H, -CH2); ^{13}C NMR data (δ ppm, DMSO-d_6): 163.38 (1C, C=O); 162.22 (1C, C=N); 149.07 (1C, C- NO_2); 139.08 (1C, C-NO_2); 134.16 (1C, Ar-C-NH); 130.66-114.84 (9C, Ar-C); 98.12 (1C, -CH_2). Mass spectral data (m/z): 342.08 (M+1).

Table 1: Physical data of synthesised compounds 4-(substituted phenylhydrazono)-6-substituted- 3,4- dihydroquinolin-2 (1*H*)-ones

Compound	R	R'	Molecular formula	Molecular weight	Melting point °C	% yield	Rf value	Solubility
IIIa_1	H	H	$C_{15}H_{13}N_3O$	251.11	>300	82.09	0.39	DMSO
IIIa_2	H	3-F	$C_{15}H_{12}N_3OF$	269.10	>300	80.09	0.41	DMSO
IIIa_3	H	3-NO_2	$C_{15}H_{12}N_4O_3$	296.28	>300	83.90	0.43	DMSO
IIIa_4	H	2,4-dinitro	$C_{15}H_{11}N_5O_5$	341.28	>300	85.90	0.45	DMSO
IIIb_1	Cl	H	$C_{15}H_{12}N_3OCl$	285.73	>300	83.79	0.41	DMSO
IIIb_2	Cl	3-F	$C_{15}H_{11}N_3OClF$	303.72	>300	81.28	0.43	DMSO
IIIb_3	Cl	3-NO_2	$C_{15}H_{12}N_4O_3Cl$	330.73	>300	84.30	0.45	DMSO
IIIb_4	Cl	2,4-dinitro	$C_{15}H_{10}N_5O_5Cl$	375.72	>300	86.50	0.47	DMSO
IIIc_1	F	H	$C_{15}H_{12}N_3OF$	269.10	>300	81.09	0.49	DMSO
IIIc_2	F	3-F	$C_{15}H_{11}N_2OF_2$	287.26	>300	80.18	0.51	DMSO
IIIc_3	F	3-NO_2	$C_{15}H_{12}N_4O_3F$	314.27	>300	81.50	053	DMSO
IIIc_4	F	2,4-dinitro	$C_{15}H_{10}N_5O_5Cl$	359.27	>300	85.80	0.55	DMSO

DMSO: Dimethyl sulfoxide, Rf: Retention factor

Elemental analysis: $C_{15}H_{12}N_4O_3$: Calculated: C, 52.79; H, 3.25; N, 20.52; O, 23.44; Found: C, 52.45; H, 3.23; N, 20.24; O, 23.56.

Structural integrity analysis of 1M17 using Ramachandran plot

To assess the structural integrity and stereochemical quality of the 1M17 protein model, a Ramachandran plot analysis was performed using the Maestro interface in Schrodinger software. The protein underwent refinement and energy minimization using the OPLS4 force field, followed by structural evaluation through the Protein Preparation Wizard and Structure Analysis tools. The phi (ϕ) and psi (ψ) backbone torsion angles for each amino acid residue were calculated and plotted to visualize their spatial distribution across standard conformational regions – namely, favored, additionally allowed, generously allowed, and disallowed areas, based on established stereochemical criteria. The Ramachandran plot reveals that a majority of the residues are situated in the favored (red) and allowed (yellow) regions, reflecting good conformational stability and correct folding. Only a few residues appear in the disallowed regions (marked by black triangles), indicating minimal stereochemical deviations. In addition, G-factor scores were computed to evaluate the likelihood of the torsion angles based on known structural preferences. Most residues showed G-factor values within acceptable limits, confirming that the overall backbone geometry is well within expected norms. This structural validation supports the reliability of the 1M17 model for further computational and functional analyses.

MolDock studies

In the field of drug design, MolDock is frequently used to predict how small molecules will bind to specific biological protein targets. This method enables thorough investigation of an active site and can be used for lead optimization, virtual screening, hit detection, and binding mode determination. Typically, docking is used to fit a substance into a generated model or to a recognised three-dimensional binding site, which may then be used to analyse the shape, orientation, and potential molecular interactions of the substance, such as hydrogen bonds and hydrophobic interactions. To create ligands for a particular protein target, MolDock is a powerful method. Despite being a useful tool in drug design, MolDock requires the construction of artificial models of complex structures that have a lot of flexibility and dynamics. Docking studies were performed to determine the possibility of the ligand (synthesised compound) and receptor binding by using Molegro Virtual Software.[8] The starting material for the synthesis of the title compounds was obtained following the literature.[9] The target compounds (IIIa_[1-4]/IIIb_[1-4]/IIIc_[1-4]) were initially sketched using ChemDraw Ultra 12.0. The resulting two-dimensional structures were subsequently converted into three-dimensional conformations, followed by energy minimization, and saved in MDL MolFile (mol2) format. The crystal structure of the target protein (PDB ID: 1M17) was retrieved from the RCSB PDB. Protein preparation involved the removal of water molecules, addition of polar hydrogen atoms, and elimination of co-crystallized ligands to ensure suitability for docking studies. The binding site of the co-crystallized inhibitor was identified and defined as the active site for docking analysis. MolDock of the synthesized ligands was performed using Molegro Virtual Docker (MVD) 2013 (version 6.0) following standard operating procedures. The docking outcomes were evaluated by comparing the MolDock scores and hydrogen bonding interactions of the test compounds with those of the reference ligand.

ADME studies

An effective molecule needs to be present at the target site in the body in a bioactive form for an adequate amount of time for the expected biological activities to take place, for it to be effective as a medicinal product. To produce new drugs, it is necessary to evaluate ADME at increasingly earlier stages of the discovery process, when the number of potential compounds is high but physical sample access is constrained.

ADME, and Toxicity (ADMET) prediction

Pharmaceutical experts have given a lot of attention to *in silico* modeling, as a technique for rational drug design, ADMET, and several ADMET-related prediction models have been reported. These models high throughput and low cost allow for a more efficient method of developing drugs, where the discovery of hits or the optimization of their structural elements can be guided by an ongoing study in terms of bioavailability, stability and activity. The usefulness of these tools, however, is dependent on their ability to meet needs at various stages. To establish ADME prediction of the target compounds (IIIa_[1-4]/IIIb_[1-4]/IIIc_[1-4]), *in silico* ADME studies were carried out using the PreADMET tool version 2.0 and found to be satisfactory.

Biological evaluation: *In vitro* anti-cancer activity by sulforhodamine B (SRB) assay

The synthesized derivatives for a series of 4-(substitutedphenylhydrazono)-6-substituted-3,4-dihydroquinolin-2(1*H*)-ones were tested for their *in vitro* anti-proliferative activity against HepG2 (Human HCC) cell line by SRB assay.[10-13]

$$\text{Percent growth was expressed as} = \frac{\text{Average absorbance of the test well}}{\text{Average absorbance of control well}} \times 100$$

Using the six absorbance measurements time zero, control growth [C], and test growth in the presence of drug at four

concentration levels [Ti], the percentage growth of each of the drug concentration levels was calculated.

$$\text{Percentage growth inhibition} = \frac{[Ti]}{[C]} \times 100$$

RESULTS AND DISCUSSION

Designing of analogs

A series of 4-(2-substitutedphenylhydrazono)-6-substituted-3,4-dihydroquinolin-2(1*H*)-one derivatives was synthesized through a two-step process involving oxidation and Schiff base formation [Figure 1]. The structural elucidation of synthesized intermediates and final compounds was confirmed using various spectroscopic techniques, such as UV, IR, ^{1}H NMR, ^{13}C NMR, and mass spectrometry. The physical data of the synthesized derivatives are given in [Table 1].

- Step I: Oxidation of 4-hydroxyquinolin-2(1*H*)-ones (Ia–Ic) to quinolin-2,4(1*H*,3*H*)-diones (IIa–IIc). The hydroxyquinolones were oxidized using CrO_3 in glacial acetic acid to form 2,4-diketone analogs. Absence of solubility in NaOH confirmed successful oxidation, and IR analysis revealed additional ketone carbonyl bands 1701.22 cm^{-1} alongside amide carbonyls 1658.78 cm^{-1}.
- Step II: Synthesis of Schiff base formation (IIIa-[1-4]/IIIb-[1-4]/IIIc-[1-4]). The final step involved condensation of the 2,4-dione compounds with substituted phenylhydrazines to yield 4-(2-substitutedphenylhydrazono)-3,4-dihydroquinolin-2(1*H*)-ones. IR spectra exhibited typical imine (C=N) stretches 1631.78cm^{-1}, in addition to amide (C=O), NH, and aromatic CH absorptions. ^{1}H NMR and ^{13}C NMR data were consistent with proposed structures, revealing expected shifts for hydrazone NH at 9.99 ppm and enolic CH_2 at 5.32 ppm. Mass spectrum also confirmed molecular mass of the compound IIIa_4, m/z 342.08 [M+1].

Assessment of stereochemical property of 1M17 protein

The stereochemical quality of the energy-minimized 1M17 protein structure was assessed using a Ramachandran plot generated via the Maestro interface in Schrodinger. The distribution of backbone dihedral angles (ϕ and ψ) is shown in [Figure 2], which highlights the conformational regions occupied by the amino acid residues. The analysis revealed that a substantial proportion of residues reside within the most favored regions (red areas), indicating appropriate backbone geometry and stable folding. In addition, a significant number of residues were located within the additionally allowed

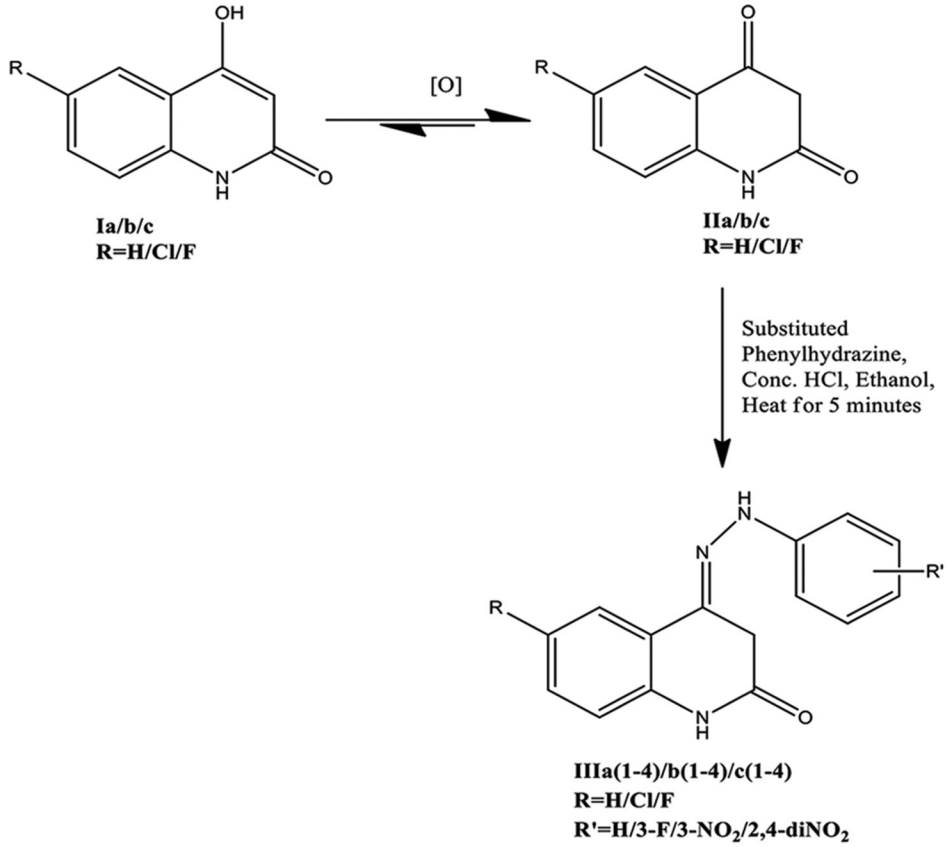

Figure 1: Scheme for synthesis of 4-(2-substitutedphenylhydrazono)-6-substituted-3,4-dihydroquinoin-2(1H)-one

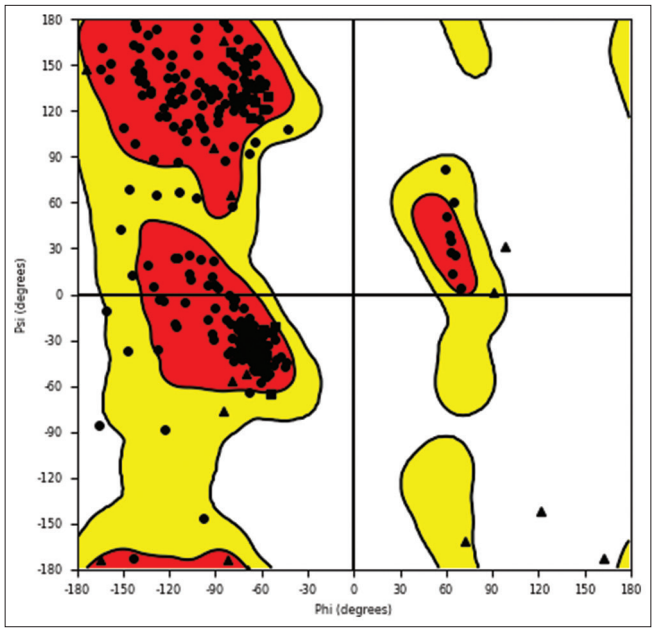

Figure 2: Ramachandran plot of the epidermal growth factor receptor kinase receptor (pdb id 1M17)

regions (yellow areas), further supporting the structural validity of the model. Only a few residues appeared in the disallowed regions, represented by black triangles, suggesting minimal geometric anomalies and no major deviations from ideal torsional angles.

The sparse occurrence of outliers in disallowed zones indicates that the protein backbone conformation adheres well to established stereochemical norms. Furthermore, G-factor evaluations yielded values within acceptable thresholds for most residues, with no significant structural outliers observed. These results collectively confirm that the 1M17 model exhibits high stereochemical integrity, making it suitable for downstream computational studies, such as MolDock and dynamic simulations.

MolDock studies

MolDock studies were conducted using MVD 6.0 to evaluate the binding affinity of synthesized derivatives (IIIa_[1–4], IIIb_[1–4], IIIc_[1–4]) towards the active site of the EGFR-TK domain (PDB ID: 1M17) as represented in [Table 2]. The MolDock scores, rerank scores, and hydrogen bonding interactions were used as parameters to assess the ligand- receptor binding efficiency. Among all tested compounds, IIIc_4 (4-(2-(2,4-dinitrophenyl)hydrazono)-6-fluoro-3,4- dihydroquinolin-2(1*H*)-one) showed the highest MolDock score of –104.42, indicating strong binding affinity, and surpassed the standard drug Adriamycin (MolDock score –76.67) in docking efficiency. This compound also exhibited the highest number of hydrogen bonding interactions (–7.30), further supporting its strong interaction with the EGFR kinase domain.

Table 2: Molecular docking studies of synthesized compounds (IIIa_[1-4]/IIIb_[1-4]/IIIc_[1-4]) using Molegro Virtual Docker 2013, 6.0

Compound	Molecular Docking score	Rerank score	H Bond
IIIa_1	–82.64	–70.13	–1.93
IIIa_2	–89.57	–73.77	–1.85
IIIa_3	–94.09	–75.92	–1.35
IIIa_4	–103.17	–59.81	–3.45
IIIb_1	–79.28	–57.14	–2.50
IIIb_2	–87.24	–53.49	–2.50
IIIb_3	–94.09	–75.78	–3.38
IIIb_4	–97.09	–57.99	–2.72
IIIc_1	–81.74	–65.22	–1.09
IIIc_2	–86.35	–66.07	–2.50
IIIc_3	–94.34	–68.05	–1.94
IIIc_4	–104.42	–32.84	–7.30
Active Ligand	–126.19	–93.69	–5.40
Imatinib	–109.39	–84.44	–0.61
Adriamycin	–76.67	–69.34	–8.20

Compounds IIIa_4 and IIIb_4, bearing the 2,4-dinitrophenyl moiety, also demonstrated high MolDock scores of –103.17 and –97.09, respectively. These values are comparable to the reference drug Imatinib (MolDock score –109.39), indicating potential for effective EGFR inhibition. The detailed analysis of receptor-ligand interactions revealed that the key residues involved in binding include Thr 766, Thr 830, Glu 738, Asp 831, Phe 832, and Met 769, which formed hydrogen bonds with the hydrazone nitrogen, quinolinone NH, and carbonyl oxygen groups of the ligands. The introduction of electron-withdrawing substituents such as fluoro and chloro at the 6-position of the quinolinone ring, as well as ortho- and para-nitro groups on the hydrazone phenyl ring, appeared to enhance binding affinity and hydrogen bonding interactions. Overall, the docking results align well with the *in vitro* anticancer activity, particularly for compounds IIIa_4, IIIb_4, and IIIc_4, further validating the EGFR-TK as a potential molecular target for these derivatives. The Mol. Dock score of the compounds along with the standard ligand is shown in [Table 2]. The figures of compound and receptor bindings are shown in [Figure 3a-f].

Biological evaluation: *In vitro* anti-cancer activity by SRB assay

The synthesized 4-(substitutedphenylhydrazono)-6-substituted-3,4-dihydroquinolin-2(1H)-one derivatives (IIIa_[1–4], IIIb_[1–4], IIIc_[1–4]) were evaluated for their anticancer activity against the hepatocellular carcinoma G2 (Hep-G2) (human HCC) cell line using the SRB assay. Each compound was tested at four different concentrations (10, 20,

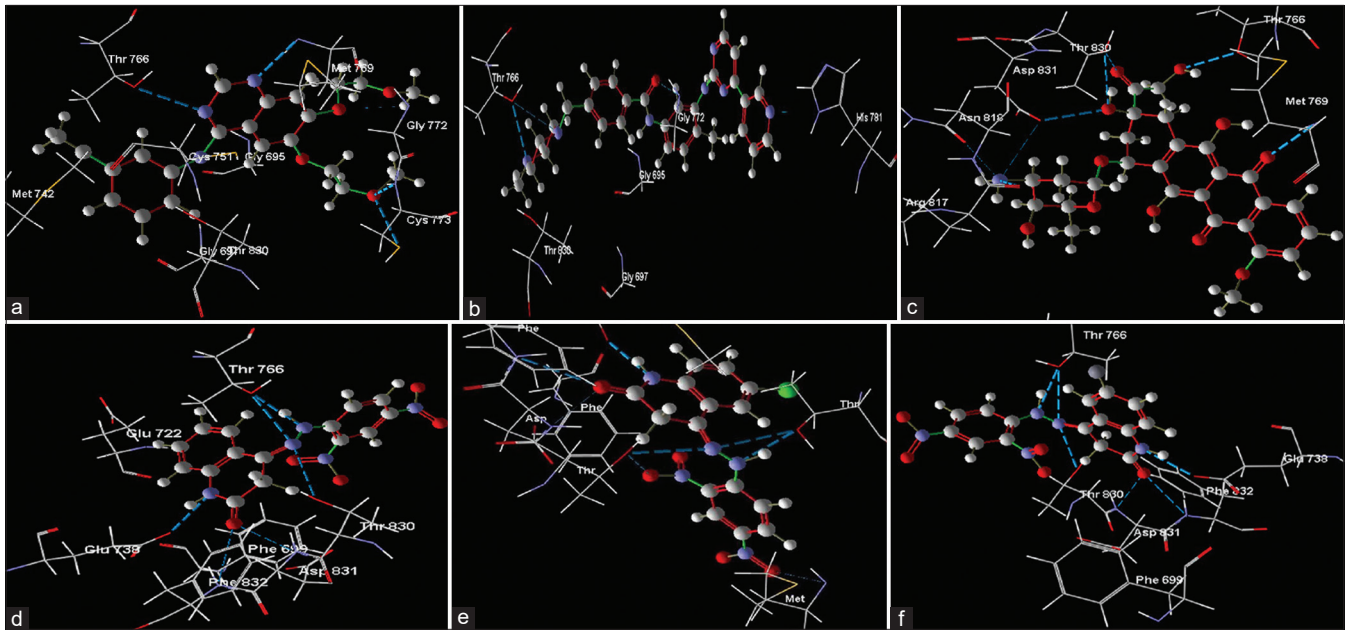

Figure 3: (a) Ligand 4-anilinoquinazoline docked in its best conformation (pose) into the binding site of 1m17. (Note: N atom at 2nd position of quinazoline moiety shows hydrogen bonding with nitrogen of Met 769; N atom at 3rd position of quinazoline moiety shows hydrogen bonding with Oxygen of Thr 766; O atom from terminal methoxy group in the 1st side chain interacts with sulfur and nitrogen of Cys 773; O atom attached to 2nd side chain of quinazoline moiety interacts with nitrogen of Gly 772). (b**)** Imatinib docked in its best conformation (pose) into the binding site of 1m17. (Note: Reference drug Imatinib shows 4 interactions with the binding site of 1m17: Oxygen of carbonyl group forms a hydrogen bond with Nitrogen of Gly 772; N atom of pyridine shows hydrogen bonding interaction with Nitrogen of His 781; Nitrogen at 1st and 4th position of piperazine shows hydrogen bonding interaction with Oxygen of Thr 766). (c) Adriamycin docked in its best conformation (pose) into the binding site of 1m17. (Note: Standard drug Adriamycin shows eight interactions with the binding site of 1m17:Oxygen of carbonyl group at 1st position of cyclohexane-1,4-dione interacts with Nitrogen of Met 769; Oxygen of hydroxy group at 1st position of hydroquinone forms hydrogen bond with Oxygen of Thr 830 and Asp 831; Oxygen of acetyl carbonyl group shows hydrogen bonding interaction with Oxygen of Thr 830; Oxygen of aliphatic hydroxy group forms hydrogen bond with Oxygen of Thr 766; Nitrogen of amino group at 4th position of tetrahydro-2H-pyran interacts by formation of hydrogen bond with Oxygen of Arg 817, Asp 831 and Asn 818). (d) 4-(2-(2,4-Dinitrophenyl)hydrazono)-3,4-dihydroquinolin-2(1*H*)-one (IIIa_1) docked in its best conformation (pose) into the binding site of 1m17. (Note: N atom of 1st and 2nd position of phenylhydrazone forms hydrogen bonds with Oxygen of Thr 766; Oxygen of Carbonyl group at 2nd position of quinolone forms hydrogen bonds with Nitrogen of Asp 831 and Phe 832; Nitrogen at 1st position of quinolone forms hydrogen bond with Oxygen of Glu 738; N atom at 1st position of phenylhydrazone forms hydrogen bond with Oxygen of Thr 830). (e) 6-Chloro-4-(2-(2,4-dinitrophenyl)hydrazono)-3,4-dihydroquinolin-2(1*H*)-one (IIIb-4). (Note: Nitrogen at 1st position of quinolone forms hydrogen bond with Oxygen of Glu 738; Oxygen of Carbonyl group at 2nd position of quinolone forms hydrogen bonds with Nitrogen of Phe 832; N atom of 1st position of phenylhydrazone forms hydrogen bonds with Oxygen of Thr 766 and Thr 830; N atom of 2nd position of phenylhydrazone forms hydrogen bonds with Oxygen of Thr 766; Oxygen of nitro group at 2nd position of phenyl ring in phenylhydrazone forms hydrogen bonds with Oxygen of Thr 830; Oxygen of nitro group at 4th position of phenyl ring in phenylhydrazone forms hydrogen bonds with Nitrogen of Met 769). **(**f) 4-(2-(2,4-Dinitrophenyl)hydrazono)-6-fluoro-3,4-dihydroquinolin-2(1*H*)-one (IIIc_4). (Note: N atom of 1st and 2nd position of phenylhydrazone forms hydrogen bonds with Oxygen of Thr 766; N atom at 1st position of phenylhydrazone forms hydrogen bond with Oxygen of Thr 830; Nitrogen at 1st position of quinolone forms hydrogen bond with Oxygen of Glu 738; Oxygen of the carbonyl group at 2nd position of quinolone forms hydrogen bonds with Nitrogen of Asp 831 and Phe 8)

40, and 80 µg/mL), and the percentage growth inhibition was determined relative to the control and is reported in [Table 3]. The lethal concentration 50%, total growth inhibition, growth inhibition 50% (GI_{50})value of each drug against each cell type was graphically calculated from a dose-response curve that was shown as percentage in [Table 4]. The dose-response curve of synthesized compounds affecting the anticancer activity is shown in [Figure 4]. Among the tested compounds, three derivatives demonstrated potent antiproliferative activity with GI_{50} values <10 µg/mL:

- IIIa_4: 4-(2-(2,4-dinitrophenyl)hydrazono)-3,4-dihydroquinolin-2(1*H*)-one
- IIIb_4: 6-chloro-4-(2-(2,4-dinitrophenyl)hydrazono)-3,4-dihydroquinolin-2(1*H*)-one
- IIIc_4: 4-(2-(2,4-dinitrophenyl)hydrazono)-6-fluoro-3,4-dihydroquinolin-2(1*H*)-one.

These compounds showed comparable cytotoxicity to the reference drug Adriamycin**,** which also exhibited a GI_{50} <10 µg/mL. The high potency of these three molecules can

Table 3: Percentage control growth of Hep-G2 cell line on treatment with the test compounds

Compound	Human Hep-G2 cell line															
	Percentage control growth															
	Drug concentrations (μg/mL)															
	Experiment 1				Experiment 2				Experiment 3				Average values			
	10	20	40	80	10	20	40	80	10	20	40	80	10	20	40	80
IIIa_1	102.9	101.3	88.7	61.8	135.7	125.6	107.7	83.9	125.4	112.4	106.1	79.1	121.4	113.1	100.8	74.9
IIIa_2	78.7	78.1	71.7	57.3	93.3	95.8	87.1	74.0	102.1	102.2	91.9	71.9	91.4	92.1	83.5	67.7
IIIa_3	98.0	88.0	78.0	63.6	106.0	104.9	95.0	74.1	103.4	101.0	90.1	79.5	102.5	98.0	87.7	72.4
IIIa_4	−6.8	−7.3	−6.1	−23.8	−10.1	−7.3	−6.1	−19.4	−1.7	−10.5	−13.4	−21.2	−2.8	−8.4	−11.9	−21.5
IIIb_2	79.4	75.3	60.1	17.0	97.3	96.0	80.4	38.7	102	93.0	79.8	48.0	93.2	88.1	73.4	34.5
IIIb_3	91.14	88.54	65.8	36.11	97.45	99.08	86.84	61.88	100	95.51	81.38	50.22	96.19	94.38	78.01	49.41
IIIb_4	−43.4	−11.4	−25.2	−22.2	−36.7	−44.3	−9.13	−18.6	−52.1	−6.90	−11.6	−19.7	−44.0	−0.03	−15.3	−20.2
IIIc_2	101.4	99.5	81.6	70.1	95.9	83.8	81.0	67.5	106.8	104.1	97.1	80.9	101.4	95.8	86.6	72.8
IIIc_3	104.8	99.5	81.6	70.1	95.9	83.8	81.0	67.5	106.8	104.1	97.1	80.9	101.4	95.8	86.6	72.8
IIIc_4	104.8	105.6	97.9	86.8	108.2	101.5	101.1	96.9	68.9	120.7	106.4	107.0	93.9	109.3	101.8	96.9
Adriamycin	−40.4	−47.9	−48.5	−43.1	−49.2	−53.8	−50.3	−37.9	−52.7	−54.6	−51.1	−38.1	−47.4	−52.1	−50.0	−39.7

Hep-G2: Hepatocellular carcinoma G2

Table 4: *In vitro* results of synthesised compounds on human Hep-G2 cell line

Compound	Human hepatoma cell line Hep-G2		
	Drug concentration (µg/mL) calculated from graph		
	LC_{50}	TGI	GI_{50}
IIIa_1	NE	NE	>80
IIIa_2	NE	NE	>80
IIIa_3	NE	NE	>80
IIIa_4	NE	**<10**	**<10**
IIIb_2	NE	NE	63.7
IIIb_3	NE	NE	79.9
IIIb_4	**>80**	**40.41**	**<10**
IIIc_2	NE	NE	>80
IIIc_3	NE	NE	>80
IIIc_4	NE	NE	**<10**
Adriamycin	**<10**	**<10**	**<10**

Hep-G2: Hepatocellular carcinoma G2, NE: Non-evaluable data, LC_{50}: Concentration of drug causing 50% cell kill, GI_{50}: Concentration of drug causing 50% inhibition of cell growth, GI_{50} value of ≤10 µg/mL is considered to demonstrate activity in case of pure compounds. For extracts, GI_{50} value ≤20 µg/mL is considered to demonstrate activity. TGI: Concentration of drug causing total inhibition of cell growth. Bold values in columns indicate compounds with significant anticancer activity.

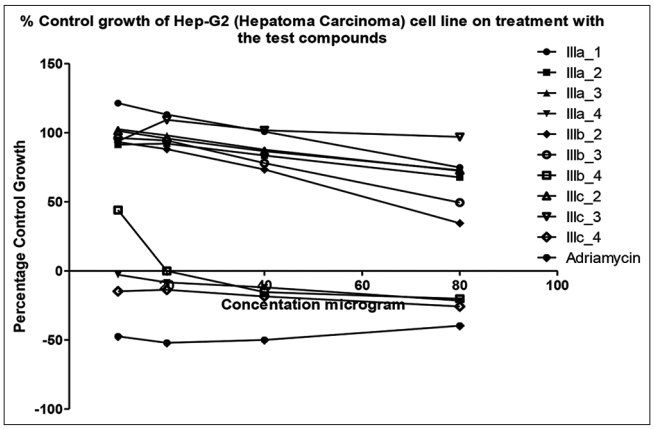

Figure 4: Graph of % control growth versus drug concentration (µg/mL)

be attributed to the presence of strong electron-withdrawing groups (two nitro groups) at ortho and para positions of the hydrazone phenyl ring, which may enhance their interaction with cellular targets. In contrast, compounds bearing single nitro or fluoro substituents at the meta position, like IIIa_3, IIIb_2, and IIIc_2, displayed moderate to low activity (GI_{50} values >60 µg/mL). Other analogs, such as IIIa_1, IIIa_2, IIIb_1, IIIc_1, and IIIc_3, showed minimal or no significant cytotoxic effects with GI_{50} values >80 µg/mL. The effects of screened compounds {IIIa(1-4); IIIb(1-4); IIIc(1-4)} on cytotoxicity of human HCC (Hep-G2)cell line at a concentration of 100 µM. The data suggest a clear structure-activity relationship, where the presence of halogens (F/Cl) at the 6-position of the quinolinone ring, combined with ortho-para dinitro substitutions on the hydrazone moiety, plays a critical role in enhancing anticancer activity. This is consistent with the docking results, in which these same compounds demonstrated the most favorable binding to the EGFR-TK domain. Thus, compounds IIIa_4, IIIb_4, and IIIc_4 emerge as promising lead molecules for further development as EGFR-targeting anticancer agents for HCC.

CONCLUSION

The research work is focused on the synthesis and characterization of a new class of 4-(2- substitutedphenylhydrazono)-6-substituted-3,4-dihydroquinolin-2(1*H*)-one derivatives and their potential as an anticancer agents were assessed through MolDock and *in vitro* cytotoxicity studies. The docking analysis against EGFR-TK (PDB ID: 1M17) indicated strong ligand-receptor interactions, particularly for compounds incorporating halogen and dinitro substitutions. Biological screening against the Hep-G2 cell line identified compounds IIIa_4, IIIb_4, and IIIc_4 as the most effective analogs, exhibiting significant cytotoxicity with GI_{50} values below 10 µg/mL. These compounds also demonstrated superior docking scores and favorable hydrogen bonding interactions with key residues in the EGFR active site, supporting their potential mechanism of action as kinase inhibitors. The combined computational and biological data suggest that these hydrazinoquinoline derivatives, especially those with electron-withdrawing substituents, hold promise as lead structures for further development in liver cancer therapy targeting EGFR. Future studies may focus on their detailed mechanism, selectivity, and *in vivo* efficacy to validate their therapeutic utility.

ACKNOWLEDGMENT

The authors are sincerely thanks to the Honorary Director, Sophisticated Analytical Instrumentation Facility (SIEF), Central Instrumentation Laboratory (CIL), Panjab University, Chandigarh, Panjab, India, for carrying the spectral analysis of synthesised compounds and Director, Advanced Centre for Treatment Research and Education in Cancer (ACTREC), Tata Memorial Centre, Navi Mumbai, Maharashtra, India for carrying out anticancer activity studies. Authors are also thankful to the Principal and Management Members of P.E.S's Rajaram and Tarabai Bandekar College of Pharmacy, Farmagudi, Ponda, Goa, India, for availing the necessary laboratories facilities to complete the present work.

REFERENCES

1. Zheng S, Chan SW, Liu F, Liu J, Chow PK, Toh HC, *et al*. Hepatocellular carcinoma: Current drug therapeutic

status, advances and challenges. Cancers (Basel) 2024;16:1582.
2. Le Grazie M, Biagini MR, Tarocchi M, Polvani S, Galli A. Chemotherapy for hepatocellular carcinoma: The present and the future. World J Hepatol 2017;9:907-20.
3. Stamos J, Sliwkowski MX, Eigenbrot C. Structure of the epidermal growth factor receptor kinase domain alone and in complex with a 4-anilinoquinazoline inhibitor. J Biol Chem 2002;227:46265-72.
4. Soares GA, Bhattacharya T, Mamledesai S, Ai Z, Hasan AM, Cavalu S. Identification of linomide derivatives as potential anticancer therapeutics using molecular docking studies. Front Pharmacol 2022;13:1-10.
5. Fonseca V, Chandavarkar S, Dabholkar R, Dessai G, Deshpande M, Shivalingrao M, *et al*. Design, synthesis of 4-[2-(substituted phenyl) hydrazono]-3-(1-hydroxyethyl)-1- phenyl/methyl-3,4-dihydroquinolin-2(1H)-one derivatives and evaluation of their in vitro tyrosine kinase inhibitor activity. Indian J Chem Sect B 2021;60:267-72.
6. Weidenfeld J, Karussis D, Abramsky O, Lehmann D, Arbell I, Ovadia H. Linomide activates the adrenocortical axis in the rat: Inhibition of experimental autoimmune encephalomyelitis by linomide is not related to the increase of corticosterone. J Neuroimmunol 1997;79:49-53.
7. Borgström P, Torres Filho IP, Vajkoczy P, Strandgården K, Polaçek J, Hartley-Asp B. The quinoline-3-carboxamide linomide inhibits angiogenesis *in vivo*. Cancer Chemother Pharmacol 1994;34:280-6.
8. Palkar MB, Praveen DM, Ronad PM, Rane RA, Patel HM, Jain KS, *et.al*. Novel series of phenylalanine analogs endowed with promising anti-inflammatory activity: Synthesis, pharmacological evaluation, and computational insights. Med Chem Res 2014;24:1988-2004.
9. Ferretti MD, Neto AT, Morel AF, Kaufman TS, Larghi EL. Synthesis of symmetrically substituted 3,3-dibenzyl-4-hydroxy-3,4-dihydro-1H-quinolin-2-ones, as novel quinoline derivatives with antibacterial activity. Euro J Chem 2014;81:253-66.
10. Vichai V, Kirtikara K. Sulforhodamine B colorimetric assay for cytotoxicity screening. Nat Protoc 2006;1:1112-6.
11. Kode J, Kovvuri J, Nagaraju B, Jadhav S, Barkume M, Sen S, *et al*. Synthesis, biological evaluation, and molecular docking analysis of phenstatin based indole linked chalcones as anticancer agents and tubulin polymerization inhibitors. Bioorg Chem 2020;105:104447.
12. Kholiya F, Chatterjee S, Bhojani G, Sen S, Barkume M, Kasinathan NK, *et al*. Seaweed polysaccharide derived bioaldehyde nanocomposite: Potential application in anticancer therapeutics. Carbohydr Polym 2020;240:116282.
13. Skehan P, Storeng R, Scudiero D, Monks A, McMahon J, Vistica D, *et al*. New colorimetric cytotoxicity assay for anticancer-drug screening. J Natl Cancer Inst 1990;82:1107-12.

Source of Support: Nil. **Conflicts of Interest:** None declared.